Contents lists available at ScienceDirect

Cement and Concrete Research

journal homepage: www.elsevier.com

NMR observation of water transfer between a cement paste and a porous medium

M. Fourmentin [a, c], P. Faure [a], S. Rodts [a], U. Peter [b], D. Lesueur [c], D. Daviller [d], P. Coussot [a, *]

[a] Université Paris-Est, Laboratoire Navier (ENPC-IFSTTAR-CNRS), Champs sur Marne, France
[b] LHOIST Recherche et Développement, Nivelles, Belgium
[c] LHOIST France, Paris, France
[d] BCB Lhoist Sud Europe, Besançon, France

ARTICLE INFO

Article history:
Received 15 April 2016
Received in revised form 10 November 2016
Accepted 24 February 2017
Available online xxx

ABSTRACT

We show that it is possible to follow the liquid transfer between a cement paste and a porous medium in contact with it, by analysing the evolution of the distribution of ^{1}H NMR relaxation times. This in particular makes it possible to see that whatever the initial water fraction in the paste, a porous medium with sufficiently small pores can rapidly extract a significant amount of water from this paste. Afterwards, during the hydration process, the cement paste progressively gets water back from this porous medium. The amount of water thus extracted by the paste finally appears to just compensate the volume loss due to water consumption by the hydration process.

1. Introduction

How liquid transfers occur between a porous medium and a cement paste is of interest for several reasons:

- It is used in internal curing which aims at mitigating autogenous shrinkage, as water in water-filled inclusions such as lightweight aggregates can supply water during cement hydration, to assist in reducing cracking [1–4];
- In hemp concrete, water transfer between the binder and hemp shives (initially saturated) can be observed [5–7] that might play a critical role in the specific hygroscopic properties of hemp concrete walls [8];
- In cement-recycled aggregates mixtures, the possible extraction of water from the paste during material preparation can have an impact on the rheological properties of the fresh matrix which can affect the setting up of the material;
- Water retention additives are often used to limit water absorption by porous substrates (typically bricks) in contact with the paste, but the origin of the effect is still debated [9–12] and our knowledge of the simple process of water extraction from a mortar (with or without additives) in contact with a porous medium is limited.

Neutron tomography [4,13–14] possibly in addition to X-ray tomography [14] are techniques that were used to study directly water transfer between a porous medium and a cement paste. In those cases, the water content was deduced from a thorough analysis of 2D pictures of the signal attenuation, which are considered as the apparent density distribution in cross-sections of the sample. It was in particular possible to observe that the water is released homogeneously from the aggregate at a significant distance from its surface (several millimetres) through the paste [13–14]. Such tomography techniques rely on the reconstruction of the distribution of local signal attenuation from a series of global attenuation measurements at various positions and along various directions. Alternatively in ^{1}H MRI (Magnetic Resonance Imaging of Hydrogen), a 3D magnetic field gradient induces a specific distribution of spin precession frequencies at different locations in the sample; this information can then be analysed to extract local characteristics of the liquid phase, as many common fluids contain hydrogen in their chemical composition. This makes it particularly useful for directly measuring the evolution of water distribution along specific directions during absorption in, or drying of, porous materials [15–20]. On the other hand ^{1}H NMR (Nuclear Magnetic Resonance) relaxometry provides the distribution of (NMR) relaxation times of hydrogen-bearing fluid molecules embedded in a sample volume that are known to depend on pore size, surface chemistry and saturation state. So far, this technique has mainly been used to study the pore characteristics of cement [21], plaster [22] or model porous systems [23–24] or more globally the structure evolution of cement or lime pastes [25–27]. However it was recently shown that NMR relaxometry can also be used to follow quantitatively the dynamics of phase transfer in composite systems such as hemp concrete [6].

Here, the water transfer between a model porous medium and a cement paste in contact with it is studied, with the help of NMR relaxometry. Materials and procedures are presented in Section 2: we used a cement paste at different W/C and clay pastes put in contact with bead packings. The experimental results, in particular the amount of water initially absorbed over a short time by the bead packing and the water amount then transferred back to the (cement) paste over longer times, are shown in Section 3. These results are further discussed in Section 4.

* Corresponding author.
Email address: philippe.coussot@ifsttar.fr (P. Coussot)

http://dx.doi.org/10.1016/j.cemconres.2017.02.027
0008-8846/

2. Material and methods

2.1. Pastes

2.1.1. Cement paste

We used a grey cement CEM I 52.5 N from Vicat. The composition and main physical characteristics of cement are described in [27]. In particular, its specific surface area was found to be 1.3 m^2/g. The particle size distribution was measured by light scattering on a Coulter LS 13320 in methanol giving a particle size distribution spreading from 1 μm to 50 μm (see [27]) with a median size around 10 μm. The cement paste was prepared by pouring the anhydrous cement in water and hand mixing during 1 min. Different water to cement ratios by mass (W/C), ranging from 0.3 to 0.63, were used. This range corresponded to materials which did not exhibit significant sedimentation when left at rest for half an hour, and can be mixed by hand without breaking in independent parts.

A cement paste is a yield stress fluid [28–29], which means that it can flow if a sufficient stress is applied on it, and acts as a solid otherwise. A yield stress can thus be defined in simple shear, which corresponds to the shear stress needed to induce the transition from the solid to the liquid regime (i.e. continuous flow). Since in addition cement pastes are thixotropic [28–30], their rheological behaviour, and in particular their yield stress, depends on the history of the flow. This for example implies that the static yield stress, which corresponds to the stress needed for flow starting from rest, will differ from the dynamic yield stress, which corresponds to the stress at flow stoppage [28–29]. Typically the static yield stress will be larger than the dynamic yield stress, since during the flow the structure somehow breaks down [31]. Moreover these two yield stress values will depend on the exact procedure (stress history) followed in each case. Here rheology measurements of these two yield stresses for our cement pastes in a wide range of W/C were obtained from a sweep test (increasing-decreasing stress ramp) (see [29]), but without applying any preshear to avoid sedimentation (the sample was placed in the rheometer just after its preparation). Both yield stresses appear to decrease strongly with increasing W/C (see Fig. 1): their variations as a function of W/C may be represented by a negative exponential function of W/C (see Fig. 6), i.e. $\tau_c = a \exp(-12.2(W/C))$ with $a = 13\,000$ Pa for the static yield stress and $a = 4550$ Pa for the dynamic yield stress.

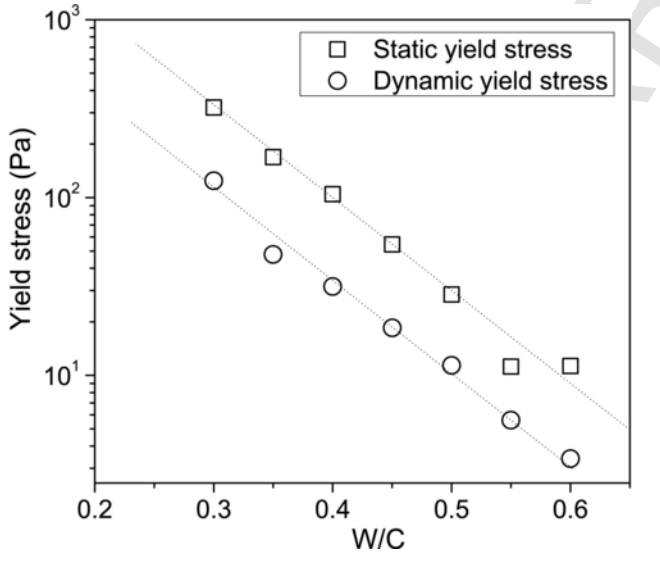

Fig. 1. Evolution of static and dynamic yield stresses of a cement paste as a function of the water to cement ratio. The dotted lines correspond to negative exponential functions fitted to data (see text) fitted to each set of data. For the largest W/C value (i.e. 0.63) reliable rheometrical data could not be obtained.

We also used cement pastes with Cellulose ethers (CE). In that aim we used methylhydroxyethyl cellulose (MHEC) of commercial name Tylose MH 100000 P6 and supplied by Shinetsu (Japan), having a degree of substitution of 1.5 and a molar degree of substitution of 0.15. They are in the form of a powder that is mixed with anhydrous cement previously to the addition of water. The samples containing cellulose ethers are then prepared under the same conditions as the samples containing simple cement pastes.

2.1.2. Other pastes

In order to confirm or test our understanding of water transfer between cement pastes and porous medium, other "pasty" materials with different internal structures were investigated. We thus used Kaolin from VWR Prolab, which is in the form of plate-like particles of diameter around 1–10 μm that develop very weak colloidal interactions when placed in water. We prepared a pasty suspension by hand-mixing Kaolin powder with water at water to solid ratio (W/S) of 0.82 (solids volume fraction of 32%). Such a paste is concentrated enough to avoid sedimentation during the measurement duration. Its measured yield stress is about 350 Pa.

A bentonite suspension was prepared from industrial grade bentonite (Impersol poudre, *Société Française des Bentonites et Dérivés*, France) mixed with water at a W/S ratio of 10 (solids volume fraction of 3.6%). The particles are deformable plate-like particles of a large aspect ratio with a length smaller than 1 μm. The suspension was first agitated continuously for about 3 h to ensure complete homogenization. It was then left to rest for at least 24 h to allow hydration and dispersion of the bentonite particles. Prior to the beginning of the experiment, the suspension was hand stirred for 2 min to ensure good handling during placement around the porous medium. At rest after mixing, it restructures so that its yield stress increases in time (see [32]). Indeed, in such a bentonite suspension, the clay particles are linked by strong colloidal interactions. The material has thus a highly thixotropic behaviour, resulting in an easy flow shortly after a strong blending, but if the material is left at rest for a sufficient time, it may exhibit a high yield stress or can develop shear-banding in some cases [33]. Here, the apparent yield stress of our paste was 50 Pa just after mixing, and 200 Pa after 30 min at rest.

We also used a standard hydrated lime CL90 S (according to EN 459-1) provided by *Lhoist* (see characteristics in [27]). This material is made of particles in the range 1 μm to 10 μm with an average particle size around 4 μm. Particles above 15 μm correspond to agglomerates of lime particles which have not been deagglomerated by ultra-sound treatment. The lime paste was prepared following the same steps as for cement, with a water to lime ratio of 0.9. The rheological behaviour of lime pastes is complex, they were shown to be thixotropic yield stress fluids with a yield stress equal to the sum of two components, one due to reversible standard colloidal interactions and one due to a brittle structure whose strength increases in time and which breaks for very small deformations [29]. For the present lime paste the (almost constant) yield stress associated with the first structure was approximately 225 Pa.

2.2. Porous media

We used packings of sintered glass beads which were prepared according to a protocol described in [34] in which the glass beads are submitted to 640 °C during 60 min. This provides a slight melting of the bead surfaces in order to bond them, yielding rigid packings.

Through this process, cylindrical samples of 35 mm diameter and 70 mm height are obtained, which are then cut to generate cubes 10 mm on a side. Such sizes are regarded as large regarding the pore size, so that cubes are true macroscopic samples with well defined homogenized porous properties (i.e they do not contain just a few beads). Additionally, since the sintering process always induce porosity gradients in the initial 70 mm column due to gravity and other thermal effects, cubes are also regarded as small enough to be considered homogeneous with respect to their local porosity and hydraulic properties. The final porosity of the sample may be adjusted via the sintering intensity. We prepared two types of such bead packings: one with a porosity of 35% (A), and one with a porosity of 26% (B), (porosity measured by dividing the volume of water required to saturate the beads by the apparent volume of the sintered beads) which respectively corresponds to a water to bead mass ratio at saturation of 0.22 and 0.12. Unless explicitly specified, all experiments were performed with beads with a diameter in the range 128 μm to 240 μm. For complementary measurements, we prepared in the same way a bead packing with larger beads of diameter ranging from 630 μm to 720 μm.

We also used a bead packing with very small hydrophilic, silica spheres (12 nm diameter). This was made following a protocol described in [35] that consists of adding salt to an initially stabilized suspension of such particles, which leads to the aggregation of the particles, thus forming a gel; then the material is slowly dried and finally most of the remaining salt is extracted by dialysis. In its final form, the solid volume fraction is 57%, close to the maximum packing fraction of a disordered uniform sphere packing (say, 62%), and the porosity is consequently about 45%.

2.3. Sample set up for water transfer measurements

The samples were placed in a NMR tube of 16 mm inner diameter. The tube was closed so that no evaporation could occur during the test. The sample height was limited to 10 mm to ensure relevant quantitative measurements of all the water present in the sample (limited region of magnetic field homogeneity). The dry porous material cube was set up at the bottom of the tube. Its top and bottom faces were covered with adhesive paper to limit the transfer through these sides. The paste was then added to fill the radial space between the cube and the tube (see Fig. 2). The paste and the porous cube then occupy each about 50% of system volume.

2.4. NMR measurements

A Bruker Minispec MQ20 ND-Series, with a 0.5 T magnetic field operating at a hydrogen resonance frequency of 20 MHz was used for NMR measurements. The probe (3 cm^3) was temperature-controlled (20 °C) by circulating water. In order to get the T_1 distribution, the full kinetics of spin-lattice relaxation, i.e. the time evolution of hydrogen longitudinal magnetization when it comes back to thermal equilibrium after an initial perturbation, was measured by means of the Inversion Recovery sequence [36], with 50 values of recovery times in the range 0.1–5000 ms. Successive measurements can be taken over several days, but each of them lasts about 30 min which means that they perform some averaging of sample characteristics over such a time. The time plotted in the different representations below corresponds to the mid time of these intervals.

As usual in porous media, it is assumed that we are in the case of a biphasic fast exchange [37], so that each local environment experienced by water molecules exhibits its own specific T_1 value. In order to resolve various T_1 possibly associated to different parts of our system, raw NMR data were processed by means of an inverse Laplace transform, so as to get the statistical distribution of T_1 in the sample. The result is expressed as a spectrum vs a T_1 axis, which typically consists of several peaks situated at different positions. The processing algorithm, similar to the 'Contin' program [38–39], is described in [25]. Note that inverse Laplace processing is unstable in nature. It suffers imperfections which prevent excessive quantitative interpretation of all features in the spectra and should be handled with care [25].

Two parameters of this distribution nevertheless constitute relevant physical characteristics of the sample: (i) the positions of the peak maxima, that we will here call the T_1 values. Roughly speaking these values are related to the mobility of water molecules, and specific interactions of these molecules with their environment. In the particular case of water embedded in a pore cavity, T_1 scales as the ratio of the volume of free liquid water to the area of the water-solid interface (mainly anhydrous cement grains, hydrates and glass) with a factor depending on the surface relaxivity that is dependent on the chemical composition of the pore surface. This volume to surface ratio is proportional to radius in the case of saturated spherical pores. Thus the T_1 values can be considered as reflecting characteristic pore sizes in a same material, as well as materials with different relativities; (ii) the area of the peak distribution, which can be correlated to the amount of water within each characteristic pore size. Note that in our case the water that reacted with anhydrous cement grains to form hydrates is no longer detectable by this technique.

3. Experimental results

3.1. Distribution of water in the different phases (paste and bead packing) when they are in contact

Here we focus on the situation obtained when a paste (either cement, kaolin, or bentonite) has just been put in contact with a porous

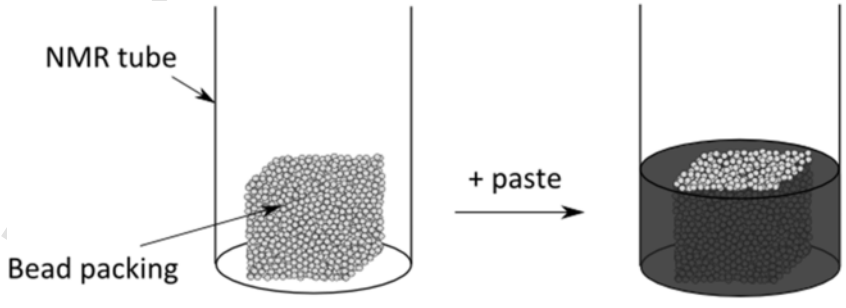

Fig. 2. Scheme of the experimental set up used for NMR measurements of transfers between sintered glass beads (cube of 9 mm of side) and a cement paste.

medium (either A or B). In any case we consider the first measure of the distribution of relaxation times. Due to the duration of such a measurement, this in fact gives us some average information about the liquid state during 30 min after this first contact. Such data thus provides a picture of the transfers which occurred during this initial period. This distribution obtained for cement paste (with porous medium A), bentonite or kaolin suspensions (with porous medium B) is shown in Fig. 3.

For all pastes, we observe a peak at low relaxation times, below 100 ms, and one or two smaller peaks between 100 and 1000 ms (see Fig. 3). The first peak is in a position similar to the main peak that can be observed for the pastes alone [27]. Additional peaks of much smaller amplitude can also be observed at much shorter relaxation times [25] but these will be neglected as they correspond to negligible amounts of water. The peaks observed here at longer relaxation times do not exist for the pastes alone because they would correspond to water in pores of a much larger size than one can find in such concentrated suspensions of micron size particles. Besides, if a significant sedimentation developed during the test, thus leading to the formation of a layer of pure water along the sample surface, we would observe a peak at a relaxation time longer than 1000 ms, as for bulk water. This means that the peaks between 100 ms and 1000 ms correspond to water inside the bead packing (this was also checked by an independent measurement of the water saturated bead packing alone). It may be suggested that the peak at the largest relaxation time could then be associated with large water volumes at the center of a packing of four to five beads in contact, while the other peak corresponds to the small volumes between beads in contact. However, NMR studies of water saturated bead packing alone usually exhibit only one single peak at an average position. The two peaks can then also just result from a spurious splitting of one single 'bead' component, a very common artefact of Inverse Laplace Transform known as 'pearling effect', which specifically affects low intensity components when another high intensity component (i.e., the paste in the present case) is present in the spectrum [25]. Further detailed interpretation of such close peaks resulting from an Inverse Laplace transform of the signal originating from a complex structure is hardly relevant.

Finally, although the sample is studied as a whole by NMR, such a distribution of relaxation times allows analysing the characteristics of water in the beads and in the cement paste separately. In particular, knowing the initial water amount in the paste, it is possible to estimate the amount of water in both porous media by measuring the area under each peak at different times after they have been put into contact. The above results also show that for any type of pastes, there is first a relatively rapid (i.e. during the first 30 min) transfer of water from the paste to the bead packing. In the following, the origin and impact of this effect will be further studied, in the case of cement paste.

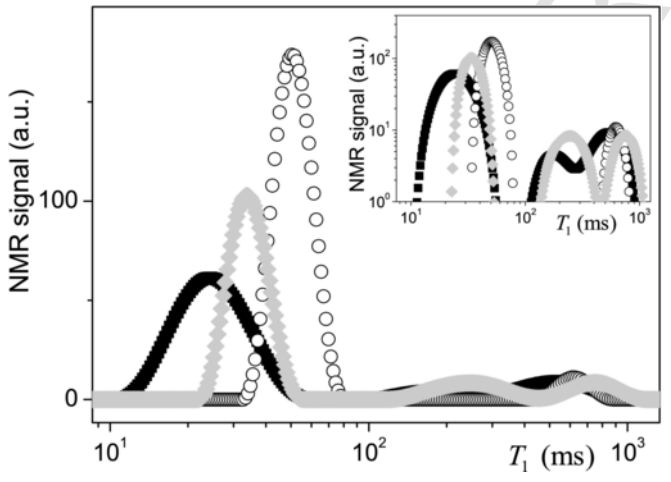

Fig. 3. Distributions of relaxation times for a paste in contact with a bead packing (A for cement, B for the two other materials) for cement paste (W/C = 0.5) (diamond), kaolin paste (squares) and bentonite paste (circles), during the first 30 min. The inset shows the same data in logarithmic scale.

3.2. Initial liquid transfer from the paste to the bead packing (first 30 min)

Let us consider again the initial situation, i.e. the first contact of a paste with a porous medium. We carried out similar tests as those described in Section 3.1 for water-cement pastes, which provided the distributions of relaxation time in these systems during the first 30 min after the first contact, but now at different initial W/C ratios and in contact with either of the porous media (A and B). The initial distribution of relaxation times are qualitatively similar to that of Fig. 3 (for cement), i.e. with a large peak at relaxation time smaller than 100 ms corresponding to water in cement paste and smaller peaks for larger relaxation times and corresponding to water in bead packing. As described above, the water volume fraction in the bead packing may be inferred from these distributions. No impact of the initial W/C ratio is observed, i.e. the amount of water transferred to the bead packing is apparently constant (despite some fluctuations due to the uncertainty on measurements) (see Fig. 4). Moreover the average value is equal (packing A) or very close (packing B) to the porosity of the bead packing, which implies that the porous media are almost entirely saturated and that this is essentially pure water which penetrated the porous medium. However, there is some significant uncertainty for the different measurements (initial porosity, water mass measured by NMR), so that one cannot exclude that there is some very small fraction of cement (paste) penetrating the porous medium either in the form of the initial paste or in the form of particles dispersed in water. This is possible because some cement particles are smaller than the largest pore size which is about 1/6 the bead diameter. In order to clarify this, samples containing cement pastes with various water to cement ratios were cut along their central plane to reveal the cement repartition in the sample. No cement particles re-

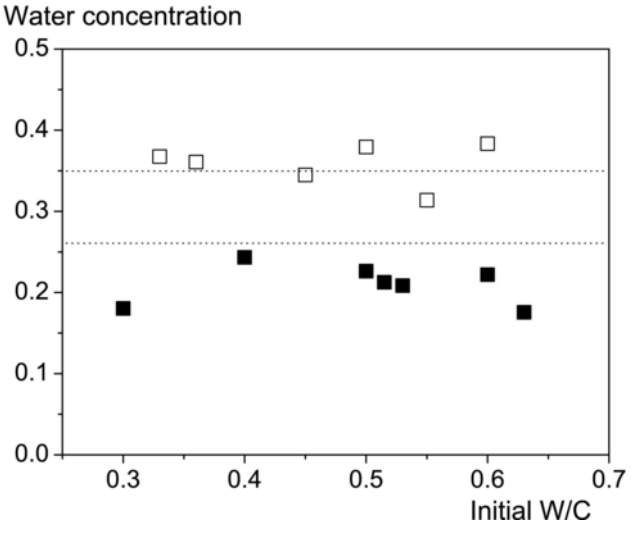

Fig. 4. Water volume fraction in the bead packing (empty squares for packing A, filled squares for packing B) after the initial period of contact with a cement paste as a function of the initial water to cement ratio of the paste. The dotted lines correspond to the porosity of each bead packing.

maining in the bead packing could be seen from direct observation (by eye) of these cross-sections which were homogeneously white. Thus, we conclude that the cement fraction penetrating the porous medium is negligible.

These results mean that, whatever the initial water to cement ratio, the bead packing extracts from the paste the amount of water this bead packing needs to be almost saturated. As a consequence, the water to cement ratio of the paste decreases, it is now equal to $(W - m_{extracted})/C$ in which $m_{extracted}$ is the mass of water transferred to the bead packing. In Fig. 5 we represent the final W/C (i.e. after the first period of contact between the paste and the bead packing) value as a function of the initial W/C for the cement paste. Since our different tests were carried out with slightly different initial ratios of paste to bead packing volume, the transferred water mass to cement ratio varies from one test to another. Moreover the porosities of the two bead packing types are different. Thus, we cannot expect a simple shift by a constant factor of W/C by this process, but we already see in Fig. 5 that our specific conditions lead to a global shift of the W/C to lower values.

3.3. Water transfer from porous medium to cement paste

Fig. 6 also presents some typical evolution of the distribution of relaxation times during the setting of the cement paste. Since after the first measurement the evolution from one measure of the distribution to the next one is slight, there is confidence that each average measurement of the relaxation time distribution over each time step well reflects the *effective* distribution during that period. We observe that the peak associated with water in the paste clearly shifts towards shorter T_1 over time. This is typical of the setting of a cement paste [27], as hydrates progressively precipitate in the pores between anhydrous cement grains. Some new thin microstructure forms in the interstitial solution, which tends to place water in smaller pores and significantly increases the amount of solid–liquid interface. As a consequence, T_1 sharply decreases from 3 h after the mixing, after the so-called induction period.

In order to follow the amount of water in the different phases we simply assume that the water in the bead packing is associated with the region of relaxation times longer than those in the high peak which corresponds to water in the paste. The evolutions of these

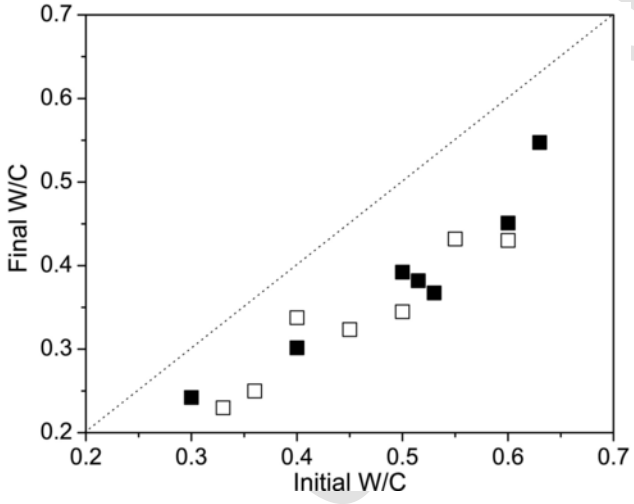

Fig. 5. "Final" W/C (i.e. after the first period of contact between the paste and the bead packing) as a function of the initial W/C for the cement paste. Empty squares for packing A, filled squares for packing B.

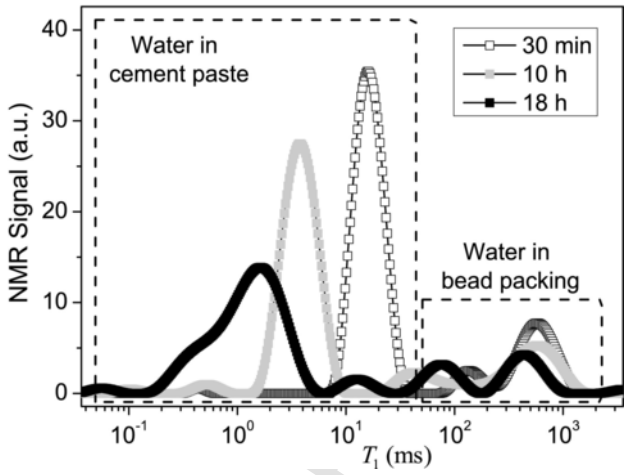

Fig. 6. Distribution of relaxation time for a cement paste (initial W/C = 0.4) in contact with a bead packing (A) at different times after the first contact. The dashed lines show the region of integration of the signal for estimating the water amount in each phase for the first distribution (i.e. 30 min).

amounts as a function of time are shown in Fig. 7 for a given W/C. The total apparent water amount in the two phases remains constant up to approximately 5 h, afterwards it starts to decrease. Since the tube containing the sample is closed, this decrease of the water amount in the bead packing means that water migrates into the paste, in which the water content should increase. However, due to cement hydration, which transforms hydrogen of liquid water into hydrogen constituting hydrates, some liquid water is "consumed" and will no longer be detectable by our NMR measurements. This means that the total (paste + bead packing) signal decrease is directly proportional to the amount of water consumed during hydration. In order to represent this water consumption, we plot the mass of consumed water (obtained as usual from the proportion of corresponding NMR signal times the initial water mass) divided by the mass of initial anhydrous cement (see Fig. 7). It is remarkable that the water starts to withdraw from the bead packing exactly when some water starts to be consumed (dashed line in Fig. 7). Note that the variations of water amount in the paste are more difficult to interpret as they result from

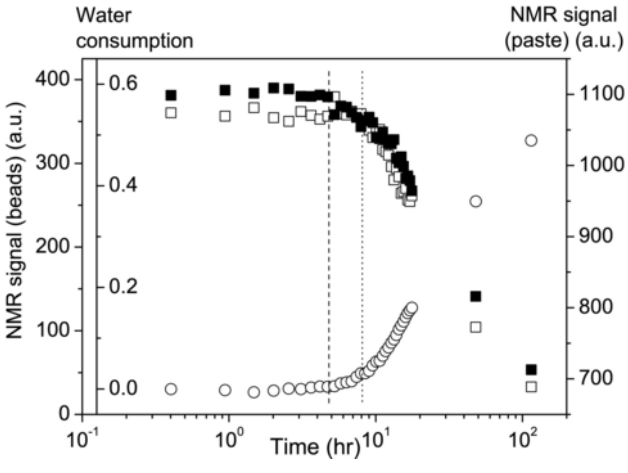

Fig. 7. Evolution of water amount in the bead packing (empty squares) and in the paste (filled squares) as a function of time elapsed since the first contact between a cement paste (W/C = 0.5) and a bead packing (A). The water consumption (see text) is represented by circles. The dashed line marks the beginning of water consumption and the dotted line the beginning of water extraction from the bead packing.

the simultaneous water arrival from the bead packing and water consumption due to cement hydration.

Under these conditions, it is interesting to compare the evolution of the mass of extracted water (from beads) to the mass of water consumed (see Fig. 8). Note that in this representation we directly used the scattered data (such as in Fig. 7) concerning the water mass evolution in the different phases with regards to the initial value. This explains that at relatively short times (i.e. for small amounts of consumed water), the values for the extracted or consumed water masses can be slightly negative. We see that, after a short period during which some water is consumed whereas there is no clear water extraction from the bead packing, the further water consumption is proportional to the water mass extracted from beads (see Fig. 8) whatever the initial conditions (in particular the W/C). This suggests that this result finds its origin in an intrinsic property of the material. More precisely this effect is certainly "imposed" by the cement paste behaviour.

4. Discussion and comparison with other systems

4.1. Flow from the paste to the bead packing

Here we review the first stage observed after putting into contact a paste and a porous medium, which corresponds to a fast water flow from the paste to the bead packing, and we analyse for each type of paste how this process can occur. We essentially consider two possibilities: i) the paste itself penetrates the porous medium, and thus brings water with it; ii) the water extracts from the paste and penetrates the porous medium alone.

4.1.1. Cement pastes

Let us first consider the possibility of penetration of the paste as a homogeneous material (particles + liquid) in the porous medium. Since the paste is a fluid, one could expect that the whole fluid itself would penetrate the bead packing as a result of capillary effects, like any liquid in contact with a dry porous medium with sufficiently small pores. However here the situation is more complex because we are dealing with a yield stress fluid, which flows only when the stress applied to it overcomes a critical value. Thus the significant penetration of the paste in the bead packing, which means that it effectively flows through it (i.e. it is not simply deformed in its solid regime), requires that the capillary stress be larger than the yield stress of the fluid. The depression induced by some liquid-air interface in the porous medium in contact with the paste may be estimated as $\Delta P = \sigma / r$, where σ is the surface tension (here taken as for water, i.e. 0.07 Pa·m), and r the typical pore size (of the order of 3.10^{-5} m). We find that a depression of the order of 2400 Pa acts on the paste. Since this value is much larger than the yield stress of all our pastes, one could expect that it would induce some flow of the paste through the porous medium. Our observations show that this is not the case (see Section 3). This is so likely because, as soon as the paste tends to penetrate the porous medium, the cement particles, which have a size around the pore size, tend to jam in the pores of the bead packing (that effectively acts as a filter).

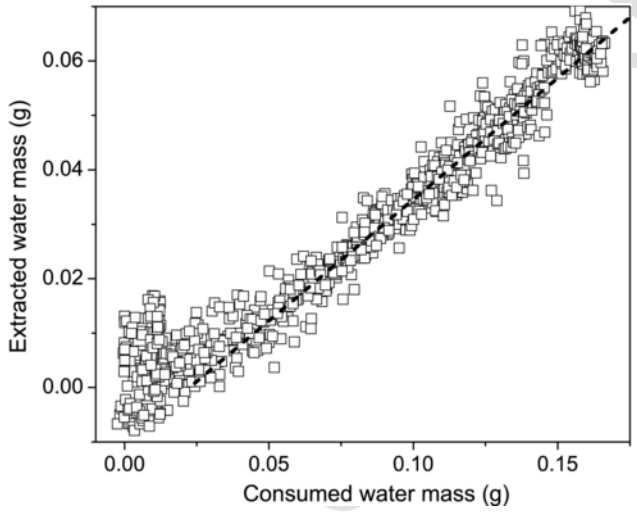

Fig. 8. Evolution of the volume of water extracted by the cement paste from beads as a function of the consumed mass for all samples with initial W/C in the range 0.3 to 0.63. The dashed line has a slope 0.43.

The other possibility is the penetration of water alone in the bead packing. If the particles are jammed around the entrance of the packing the depression acts on the water films which surrounds the particles of the paste and are in contact with the beads. This will tend to move water from the paste towards the bead packing. Here the paste may be seen as a porous medium since it has a solid structure (the network of particles in interaction at the origin of its yield stress) and is filled with a liquid. This porous medium cannot keep its shape while the water is extracted from it and replaced by air. This would indeed induce capillary forces much higher than that in the sintered bead packing, since the pore size inside the cement paste is of the order of the particle size. Moreover, these forces would be sufficient to induce a collapse of the structure (see above).

Actually, as water is withdrawn from the structure, the paste shrinks, i.e. the particles get closer to each other while some water flows outside. Such a process has two effects: (i) it induces a flow of water through the paste structure and then in the bead packing, and (ii) it induces a compression of the paste structure. For a sufficiently slow process, in order to estimate the pressure on the structure, we can neglect the pressure gradient specifically associated with the water flow through the paste and consider only the stress needed to compress the paste structure. This stress does not depend on the water velocity and may be estimated from the stress needed for a compression of the homogeneous paste (without water extraction) at low velocity, since here also it is essentially the solid structure deformation that is at the origin of the stresses developed. For a yield stress fluid in its solid regime, as for usual solids, the stress is proportional to some elastic modulus of the material and to the imposed deformation. However in general (this is observed in simple shear) the elastic modulus strongly decreases when the deformation increases. As a consequence here we will directly consider the stress associated with some deformation, and more precisely we will only consider the maximum stress (critical stress) needed to deform the material at a very small velocity. For fluids with a yield stress, the critical normal stress needed to induce a compression (keeping the volume constant) is proportional to the fluid yield stress (measured in simple shear) with a factor depending on the exact boundary conditions but which is of the order of one [31]. The rheological data of Fig. 1 show that even for the most concentrated paste, the corresponding stress (of the order of 1100 Pa for the static yield stress) is still smaller than the typical capillary pressure (see above estimation). This explains that in our range of concentrations, the water is extracted from the paste which then shrinks. Note that here we implicitly assumed that this shrinkage is homogeneous. In fact this is not so obvious considering the geometry of the system (a square in a circle), but we observed that at the end of the test the paste shape was still circular and no crack was observed. This suggests that the water flow and the paste shrinkage adapt themselves to these complex boundary conditions.

We deduce from the above analysis that the extraction of water from the paste will be possible as long as the capillary pressure is larger than the yield stress of the paste. And it will end (if we have a porous medium of large volume in contact with a paste, which thus contains enough water) when the paste yield stress associated with the new paste concentration approaches the capillary pressure. For example, in our case it would likely be possible to induce a decrease of W/C for initially liquid pastes (say, with W/C around 0.5) down to values of the order of 0.3, by using a sufficiently large ratio of bead packing to paste volume, without fearing the developments of heterogeneities despite a larger total shrinkage of the paste.

4.1.2. Other pastes

We can test the validity of these reasonings from tests with other paste types. A similar process occurs for the kaolin paste, which is made of particles of a size not much smaller than those of a cement paste, and with a yield stress of the order of the highest values of our cement paste. A full water extraction occurs during the first 30 min. However, the process is different for the bentonite paste: the signal in the glass beads increases during the first 3 h of the experiment and then stabilizes when the water saturates the bead packing. Note that when the cube is removed from bentonite after the experiment, rinsed and cut, a penetration front of about 1 mm is clearly visible, meaning that part of the bentonite entered the beads. The evolution of the signal may then be explained by a penetration of the bentonite suspension more or less as a whole in the glass beads in the very first times. Such a penetration does not increase the signal considered to correspond to water absorption "in the beads" because the NMR signal still corresponds to water in the (pores within the) paste. In that case a penetration of the paste through the porous medium is permitted because the bentonite suspension is made of particles much smaller than those of the cement paste and thus a possible jamming of the particles in the pores of the sintered beads does not occur immediately. But additionally, the yield stress is lower than that of Kaolin paste, whose yield stress is between 50 Pa and 200 Pa, so that bentonite can actually flow through the medium due to capillary effects. After some penetration in the bead packing however, the pressure gradient needed to advance further is larger than capillary effects and the flow stops. Then the flow of water through the paste can go on, but this occurs more slowly than with a cement paste due to the lower permeability of the bentonite suspension.

We also carried out this type of test with a lime putty (with a water to lime ratio of 0.9). The water transfers was followed over several days, as characteristic times of evolution of lime structure are longer than in cement. Once again, it was possible to clearly distinguish, in the distribution of relaxation times, the NMR signal associated with water in the lime paste from that associated with water in the bead pack. We observe, as for the cement pastes, a rapid transfer of water from the paste to the bead packing, and then no more apparent change of the water amount in the porous medium. However, the T_1 associated to water in the lime putty shifts towards shorter T_1 over time. This was already observed during the aging of a lime putty and is associated to the strong structural changes happening for Portlandite crystals [27]. Thus, the beads initially absorb water from the lime putty, but the microstructural changes occurring in the lime putty during its aging are not at the origin of capillary forces, or at least not sufficient to suck up water. This is not surprising given that in the case of a lime putty, contrary to cement, no water is consumed during the chemical reaction [27].

Thus, we see that the absorption of water in the bead packing can occur in different ways depending on the structure, the permeability, the yield stress, and the capillary effects. In this context, it is finally interesting to look at the effect of cellulose ethers which are considered as water retaining agents. These products are added to mortars or plasters for example to avoid water suction by the porous substrate (typically bricks). They appear to be quite effective for this purpose, even though the mechanisms at the origin of this water retention are still under discussion [9,12]. Cellulose ethers (CE) were added to the cement paste surrounding the glass beads. The distribution of relaxation times is not modified compared to the cement paste without water retaining agents. The peaks corresponding to water in the cement paste and in the glass beads are well separated, which allows measuring the signal associated to each phase of the sample. The effect of the presence of CE in the cement paste can be observed from a comparison of the NMR signal associated to water in the bead packing for a sample with CE and the same sample without CE. In order to directly compare the evolution of the water mass in the two systems, we used similar sample volumes in that case.

The amount of water absorbed by the bead packing is much smaller with CE than without (see Fig. 9), by a factor of about 10. This effect is likely due to the clogging effect described in [9]. It was indeed shown that when a CE solution flows through a porous medium (bead packings of size between 200 μm and 600 μm), it first penetrates as expected from the balance between capillary and viscous effects. Then, after some distance of penetration, it dramatically slows down and finally apparently stops flowing as a whole (then a very slow water flow seems to persist). This effect, which was also observed in flow through sieves was attributed to a clogging of the pores by CE aggregates (note that successive filtrations do not allow removal of this effect). Finally, when the hydration reaction starts, we again observe a decrease of signal, similar to that observed without CE, but in that case it is lower since there is initially much less water in the bead packing. In this context, it is difficult to conclude about the impact of CE in the subsequent extraction of water from the bead packing.

4.2. Flow from the bead packing to the paste

At the end of the initial absorption of water (from the paste) by the bead packing, as the bead packing is saturated, the initial capillary effects have fully played their role and no further motion of liquid is expected. On the contrary we observe a significant transfer of liquid back to the paste (see Section 3). This means that there is some change inside the paste which drives this motion of liquid, and it is natural to consider that this is related to hydration since this is the basic evolution of the paste. Our results tend to indicate that, during all the process of water flow from the beads to the paste, the ratio of water extracted from the bead packing to water consumed beyond a small critical value is constant at any time and whatever the initial conditions. A similar result was found when comparing the water extracted from light weight aggregates immersed in a cement paste to volume of water associated with the chemical shrinkage accompanying cement hydration [40]. In order to understand this result we have to keep in mind that a density change is associated with cement hydration reaction. This is the Le Chatelier shrinkage/contraction, which is due to the fact that the hydrates formed during the process have a higher density than the sum of reactants that are consumed to form them. As a consequence, in the absence or air or water penetration inside the paste, we expect a shrinkage of the cement paste. In fact at the beginning of the hydration process, the yield stress of the material is in general still sufficiently low [29] for the paste to be able to shrink (so-called plastic shrinkage), so that no water is extracted from the bead packing. This corresponds to the period situated between the dashed and dotted lines in Fig. 7. In a second stage (beyond

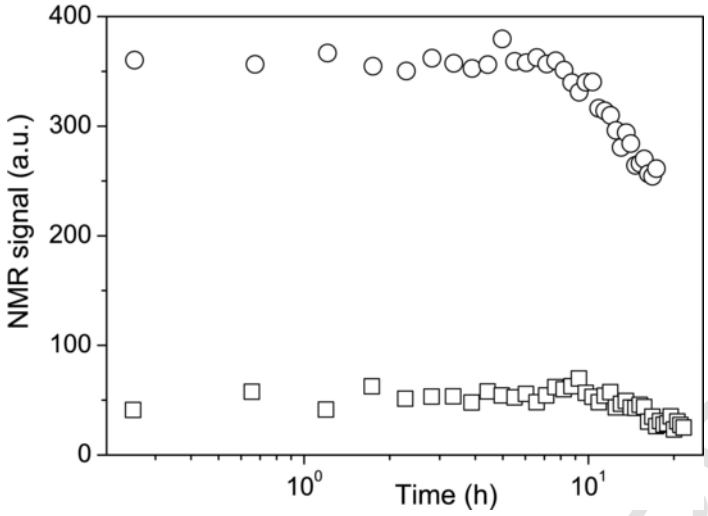

Fig. 9. Evolution of the signal associated to water in the beads in the case of a cement paste with a W/C of 0.4 in contact with sintered beads and containing cellulose ethers (filled squares) or not (open circles) over time.

the dotted line), i.e. when the structure has become strong enough it can resist capillary effects, and then some water may be extracted from the bead packing, provided suction effects in the paste become sufficient. This explains that there is a first period (between 5 h and 8 h) during which some water is consumed in the paste, but the water amount in the bead packing remains constant, while beyond 8 h some water starts to be extracted from the bead packing, in proportion to the water consumed from that time. Note that the factor of proportionality found in literature [41–42] for the ratio of extracted water (from the beads) to consumed water (i.e. 0.31) is smaller that ours (i.e. 0.43).

In fact, the process of water extraction from the bead packing implies the set-up of a pressure larger than capillary effects in the beads. This pressure may originate from the smaller pore size in the paste than in the porous media: had the paste begin to desaturate, then water/air interface at the upper surface of the paste would be pulled downward, immediately creating the necessary capillary forces in the paste to maintain saturation by pumping water in the glass-beads reservoir. However, due to the chemical reaction at work in this medium, the chemical potential of water in the paste is certainly smaller than in the bead packing so that osmotic pressure can also come into play. We ignore the value in a cement paste, as it will depend on the different species in solution, but we can consider that a typical associated pressure difference can be of the order of 10^5–10^6 Pa (just think for example that the typical osmotic pressure induced by the presence of salt in sea water is 2.6×10^6 Pa). This value is much larger than capillary effects within beads, and thus can easily induce the flow from the bead packing to the paste.

In this context, once again to test the validity of our reasonings, it is interesting to use a porous medium for which suction effects are much larger. In that aim, we replace the bead packing by a silica gel. Note that in this case of nanometre sized pores, water suction originates from both capillary and osmotic effects due to adsorption at silica surfaces. In that case, the relaxation times of water in the fresh paste and in the gel are close so that the distribution of relaxation times exhibits only one peak. When cement hydration starts, say after about 5 h, the peak associated with water in the paste shifts towards a shorter relaxation time so that it can be distinguished from the peak for water in the gel (see Fig. 10). We finally observe that the bead packing is rapidly filled with water (note that the initial increase is likely due to an artefact resulting from the difficulty to distinguish water in the different phases when the peaks are close) (see Fig. 11).

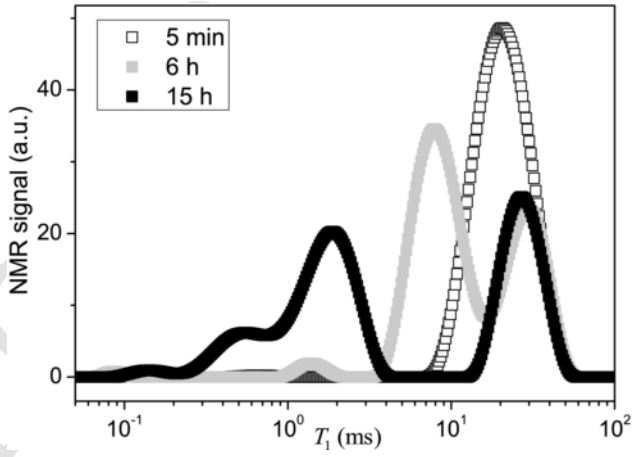

Fig. 10. Distribution of relaxation time for a cement paste (initial W/C = 0.4) in contact with a nanoporous silica gel at different times after the first contact.

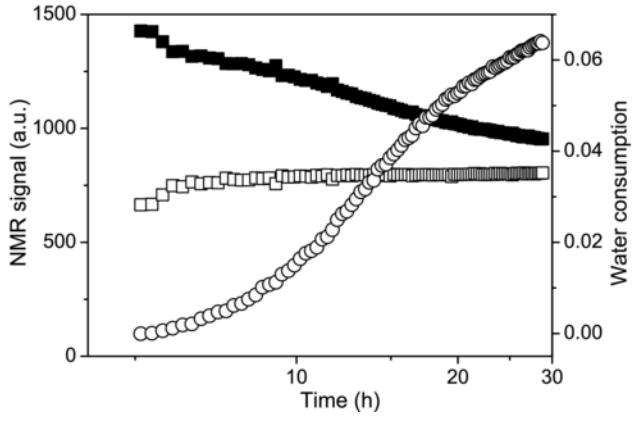

Fig. 11. Evolution of water amount in the bead packing (empty squares) and in the paste (filled squares) as a function of time elapsed since the first contact between a cement paste (W/C = 0.5) and a silica gel. The water consumption (see text) is represented by empty circles.

Then, the amount of consumed water increases in time while the mass of water in the paste decreases, but here the water mass in the gel remains constant. This result strongly contrasts with that obtained with the bead packing. Another original trend is that the water consumption is much lower than with the bead packing, after 20 h it is equal to about 0.05 instead of 0.2 for cement in contact with bead packing.

Here, we have a fast absorption of water by the gel because suction effects are higher than with a bead packing. Then, it is likely that both capillary and osmotic effects in the paste are now insufficient to induce a suction larger than that in the packing. Regarding the only capillary effects, capillary pressure in silica is of the order of 10^7 Pa, which is much larger than both typical osmotic and capillary pressures in 100 nm to 1 μm pore size (characteristic pore size in our pastes).

5. Conclusions

In this work, we showed that NMR allows to follow the liquid transfer between a cement paste and a porous medium in contact with it, by analysing the evolution of the distribution of ^{1}H NMR relaxation times. We were able to measure the amount of liquid present in each phase (paste and porous medium) at any time after they have been put in contact. We could observe that whatever the initial water fraction in the paste, a porous medium with sufficiently small pores can rapidly extract a significant amount of water from this paste. Afterwards, during the hydration process, the cement paste progressively gets water back from this porous medium. The amount of water thus extracted by the paste finally appears to simply balance the volume loss due to water consumption by the hydration process.

We thus could observe that much water can be extracted from cement whatever its initial W/C (in a range associated with real cases) but that all of this water can then be sucked back during the subsequent hydration reactions.

This technique may be used to study the impact of the different conditions of preparation of a recycled concrete, and determine the most appropriate component fractions (cement and aggregate) and the procedure (in particular concerning the interest of a pre-wetting). This can also help identifying different cement pastes, possibly better fitted to a mixture with aggregates, leading to concrete with improved mechanical properties.

Here, we finally focused on some extreme or specific situations (in terms of pore sizes of the aggregates, cement type, and available water amount). A more systematic study and understanding of the impact of the physical characteristics of the different systems, should be carried out in the future.

Acknowledgement

The authors thank Cédric Mézière for technical support, Jules Thiery for providing the nanocolloidal gels and Sandrine Gauffinet and André Nonat for fruitful discussions.

References

[1] D.P. Bentz, Early-age cracking review: mechanisms, material properties, and mitigation strategies, In: Cementitious Barriers Partnership, 2009 (CBP-TR-2009-002-C3).
[2] O. Jensen, P.F. Hansen, Water-entrained cement-based materials. I. Principles and theoretical background, Cem. Concr. Res. 31 (2001) 647–654.
[3] R. Henkensiefken, P. Briatka, D.P. Bentz, T.E. Nantung, J. Weiss, Plastic shrinkage cracking in internally cured mixtures, Concr. Int. 32 (2010) 49–54.
[4] M. Wyrzykowski, P. Trtik, P. Münch, J. Weis, P. Vontobel, P. Lura, Plastic shrinkage of mortars with shrinkage reducing admixture and lightweight aggregates studied by neutron tomography, Cem. Concr. Res. 73 (2015) 238–245.
[5] A. Arizzi, G. Cultrone, M. Brümmer, H.A. Viles, Chemical, morphological and mineralogical study on the interaction between hemp hurds and aerial and natural hydraulic lime particles: implications for mortar manufacturing, Constr. Build. Mater. 75 (2015) 375–384.
[6] P. Faure, U. Peter, D. Lesueur, P. Coussot, Water transfers within hemp lime concrete followed by NMR, Cem. Concr. Res. 42 (2012) 1468–1474.
[7] M. Fourmentin, Impact of Water Distribution and Transfers on the Properties of Lime-Based Buiding Materials, Ph.D. Univ. Paris-Est, 2015 (in French).
[8] F. Collet, M. Bart, L. Serres, J. Miriel, Porous structure and water vapour sorption of hemp-based materials, Constr. Build. Mater. 22 (2008) 1271–1280.
[9] C. Brumaud, H. Bessaies-Bey, C. Mohler, R. Baumann, M. Schmitz, M. Radler, N. Roussel, Cellulose ethers and water retention, Cem. Concr. Res. 53 (2013) 176–184.
[10] D. Bülichen, J. Kainz, J. Plank, Working mechanism of methyl hydroxyethyl cellulose (MHEC) as water retention agent, Cem. Concr. Res. 42 (2012) 953–959.
[11] A. Jenni, R. Zurbriggen, L. Holzer, M. Herwegh, Changes in microstructures and physical properties of polymer-modified mortars during wet storage, Cem. Concr. Res. 36 (2006) 79–90.
[12] C. Marlière, E. Mabrouk, M. Lamblet, P. Coussot, How water retention in porous media with cellulose ethers works, Cem. Concr. Res. 42 (2012) 1501–1512.
[13] I. Maruyama, M. Kanematsu, T. Noguchi, H. Iikura, A. Teramoto, H. Hayano, Evaluation of wáter transfer from saturated lightweight aggregate to cement paste matrix by neutrón radiography, Nucl. Inst. Methods Phys. Res. A 605 (2009) 159–162.
[14] P. Trtik, B. Münche, W.J. Weiss, A. Kaestner, I. Jerjen, L. Josic, E. Lehman, P. Lura, Release of internal curing water from lightweight aggregates in cement paste investigated by neutron and X-ray tomography, Nucl. Inst. Methods Phys. Res. A 651 (2011) 244–249.
[15] L. Pel, K. Kopinga, G. Bertram, G. Lang, Water-absorption in a fired-clay brick observed by NMR scanning, J. Phys. D. Appl. Phys. 28 (1995) 675–680.
[16] L. Pel, K. Hazrati, K. Kopinga, J. Marchand, Water absorption in mortar determined by NMR, Magn. Reson. Imaging 16 (1998) 525–528.
[17] K.M. Song, J. Mitchell, H. Jaffel, L.F. Gladden, Magnetic resonance imaging studies of spontaneous capillary water imbibition in aerated gypsum, J. Phys. D. Appl. Phys. 44 (2011) 115403.
[18] S. Gupta, H.P. Huinink, M. Prat, L. Pel, K. Kopinga, Paradoxical drying of a fired-clay brick due to salt crystallization, Chem. Eng. Sci. 109 (2014) 204–211.
[19] V. Voronina, L. Pel, K. Kopinga, Effect of osmotic pressure on salt extraction by a poultice, Constr. Build. Mater. 53 (2014) 432–438.
[20] P. Faure, P. Coussot, Drying of a model soil, Phys. Rev. E 82 (2010) 036303.
[21] P.J. McDonald, J.P. Korb, J. Mitchell, L. Monteilhet, Surface relaxation and chemical exchange in hydrating cement pastes: a two-dimensional NMR relaxation study, Phys. Rev. E 72 (2005) 011409.
[22] K.M. Song, J. Mitchell, H. Jaffel, L.F. Gladden, Simultaneous monitoring of hydration kinetics, microstructural evolution, and surface interactions in hydrating gypsum plaster in the presence of additives, J. Mater. Sci. 45 (2010) 5282–5290.
[23] J.P. Korb, S. Xu, J. Jonas, Confinement effects on dipolar relaxation by translational dynamics of liquids in porous silica glasses, J. Chem. Phys. 98 (1993) 2411–2422.
[24] R.M.E. Valckenborg, L. Pel, K. Kopinga, Combined NMR cryoporometry and relaxometry, J. Phys. D. Appl. Phys. 35 (2002) 249–256.
[25] P.F. Faure, S. Rodts, Proton NMR relaxation as a probe for setting cement pastes, Magn. Reson. Imaging 26 (2008) 1183–1196.
[26] K.M. Song, J. Mitchell, L.F. Gladden, Magnetic resonance studies of hydration kinetics and microstructural evolution in plaster pastes, J. Mater. Sci. 44 (2009) 5004–5012.
[27] M. Fourmentin, P. Faure, S. Gauffinet, U. Peter, D. Lesueur, D. Daviller, G. Ovarlez, P. Coussot, Porous structure and mechanical strength of cement-lime pastes during setting, Cem. Concr. Res. 77 (2015) 1–8.
[28] N. Roussel, G. Ovarlez, S. Garrault, C. Brumaud, The origins of thixotropy of fresh cement pastes, Cem. Concr. Res. 42 (2012) 148–157.
[29] M. Fourmentin, G. Ovarlez, P. Faure, U. Peter, D. Lesueur, D. Daviller, P. Coussot, Rheology of lime paste - a comparison with cement paste, Rheol. Acta 54 (2015) 647–654.
[30] S. Jarny, N. Roussel, S. Rodts, R. Le Roy, P. Coussot, Rheological behavior of cement pastes from MRI velocimetry, Concrete Cem. Res. 35 (2015) 1873–1881.
[31] P. Coussot, Rheometry of Pastes, Suspensions, and Granular Materials: Applications in Industry and Environment, Wiley, New York, 2005.
[32] S. Rodts, J. Boujlel, B. Rabideau, G. Ovarlez, N. Roussel, P. Moucheront, C. Lanos, F. Bertrand, P. Coussot, Solid-liquid transition and rejuvenation similari-

ties in complex flows of thixotropic materials studied by NMR and MRI, Phys. Rev. E 81 (2010) 021402.
[33] P. Coussot, H. Tabuteau, X. Chateau, L. Tocquer, G. Ovarlez, Aging and solid or liquid behavior in pastes, J. Rheol. 50 (2006) 975–994.
[34] F. Osselin, Thermochemical-Based Poroelastic Modelling of Salt Crystallization, and a New Multiphase Flow Experiment: How to Assess Injectivity Evolution in the Context of CO_2 Storage in Deep Aquifers (Ph.D. thesis) Univ. Paris-Est, 2013.
[35] J. Thiery, S. Rodts, E. Keita, X. Chateau, P. Faure, D. Courtier-Murias, T.E. Kodger, P. Coussot, Water transfer and crack regimes in nanocolloidal gels, Phys. Rev. E 91 (2015) (2015) 042407.
[36] P.T. Callaghan, Principles of Nuclear Magnetic Resonance Microscopy, Clarendon Press, Oxford, 1991.
[37] S. Philippot, J.P. Korb, D. Petit, H. Zanni, Analysis of microporosity and setting of reactive powder concrete by proton nuclear relaxation, Magn. Reson. Imaging 16 (1998) 515–519.
[38] K.P. Whittall, A.L. MacKay, Quantitative interpretation of NMR relaxation data, J. Magn. Reson. 84 (1989) 134–152.
[39] S.W. Provencher, A constrained regularization method for inverting data represented by linear algebraic or integral equations, Comput. Phys. Commun. 27 (1982) 213–227.
[40] D.P. Bentz, P.M. Halleck, A.S. Grader, J.W. Roberts, in: O.M. Jensen, P. Lura, K. Kovler (Eds.), Four-Dimensional X-ray Microtomography Study of Water Movement during Internal Curing, in Proc. of the International RILEM Conference – Volume Changes of Hardening Concrete: Testing and Mitigation, RILEM Publications S.A.R.L, Bagneux, France, 2006, pp. 11–20.
[41] A.M. Neville, Properties of Concrete, Prentice Hall, Essex, 1995.
[42] F.M. Lea, The Chemistry of Cement and Concrete, Elsevier, Amsterdam, 1998.